

Deep Learning and Remote Sensing for Agricultural Land Use Monitoring: A Spatio-Multitemporal Analysis of Rice Field Conversion using Optical Satellite Images

Arie Wahyu Wijayanto ^{1*}, Bill Van Ricardo Zalukhu ², Salwa Rizqina Putri ¹, Nori Wilantika ¹, Budi Yuniarto ¹, Robert Kurniawan ¹, Ahmad R. Pratama ³

¹Department of Statistical Computing Politeknik Statistika STIS Jakarta, Indonesia

²BPS-Statistics Padang Lawas Utara Regency North Sumatera, Indonesia

³Stony Brook University New York, United States

Article Info

Article history:

Received May 18, 2025

Revised May 28, 2025

Accepted Jun 30, 2025

Keywords:

Remote Sensing

Deep Learning

Use Change

Paddy Field Monitoring

Sustainable Agriculture

ABSTRACT

Rice is a staple food for over half of the global population, making its production crucial for food security, especially in Indonesia, the world's third-largest rice consumer. Population growth and urban expansion have led to agricultural land conversion, necessitating efficient monitoring methods. Traditional approaches, such as area sample frameworks and tile surveys, are costly and time-consuming, prompting the need for remote sensing and deep learning solutions. This study utilizes medium-resolution Sentinel-1, Sentinel-2, and Landsat-8 optical satellite imagery from 2013 and 2021 to analyze land cover changes in West Bandung and Purwakarta Regencies, key agricultural regions in Indonesia. A deep learning model is developed to classify land cover, validated through ground-truth evaluation, and applied to assess spatio-multitemporal land use conversion, paddy field estimation, and conversion rates. Results show that deep learning models effectively classify land cover with high accuracy, revealing significant agricultural land loss due to urban expansion. This research contributes to artificial intelligence (AI)-driven land monitoring, particularly in tropical regions, and supports policymakers in sustainable food agriculture land management. The findings highlight the potential of integrating remote sensing and deep learning for cost-effective agricultural monitoring, ensuring food security and sustainable land use. Future research should explore higher-resolution imagery and advanced AI techniques to enhance predictive accuracy and decision-making.

This is an open access article under the [CC BY-SA](https://creativecommons.org/licenses/by-sa/4.0/) license.



Corresponding Author:

Arie Wahyu Wijayanto,
Department of Statistical Computing
Politeknik Statistika STIS
Jakarta, Indonesia.
Email : ariewahyu@stis.ac.id

1. INTRODUCTION

Rice is widely recognized as one of the most essential agricultural commodities, serving as the primary staple for more than half of the global population—approximately three billion people [1]. During the 2021–2022 period, global rice consumption reached an estimated 509.87 million metric tons. Given its critical role in sustaining food systems and livelihoods, rice production is

fundamentally linked to global food security. This significance directly aligns with the United Nations Sustainable Development Goal (SDG) 2: “Zero Hunger,” which emphasizes the need to end hunger and ensure access to safe, nutritious, and sufficient food for all [2]. Indonesia has the world's third-biggest rice consumption, hence agriculture has evolved into a critical aspect to be aware of [3]. Furthermore, the majority of individuals make their livelihood in the agricultural sector. The increasing population and per capita consumption, primarily driven by rising household incomes, have led to a growing demand for rice. To maintain equilibrium and ensure food security, national rice production is expected to expand accordingly. Additionally, population growth has accelerated the development of non-agricultural economic infrastructure, contributing to the conversion of agricultural land for alternative uses. This shift underscores the necessity of comprehensive land-use monitoring to balance agricultural sustainability—particularly rice cultivation—with the rising demand for non-agricultural land. However, resource constraints have posed significant challenges to the effective implementation of such monitoring efforts.

Statistics Indonesia (BPS) routinely publishes official data on harvested area and rice productivity to monitor the development of rice production across the country. Harvested area figures are derived using the Area Sample Framework (ASF) method during the last seven days of each month, while productivity estimates are obtained through tile surveys conducted during harvest periods. However, these conventional methods are often constrained by high operational costs, intensive labor requirements, and time-consuming procedures. To address these limitations, the adoption of cost-efficient data acquisition technologies—such as remote sensing—is strongly encouraged by international organizations including the United Nations Statistical Division (UNSD), the Food and Agriculture Organization (FAO), and the Asian Development Bank (ADB). Remote sensing is defined as the science and art of obtaining information about objects, areas, or phenomena through the analysis of data acquired without direct physical contact [4]. This technology offers a time-efficient and highly accurate means of producing integrated and comprehensive land cover data, thereby facilitating effective monitoring of land use and conversion dynamics [5], [6]. Despite its potential, the application of satellite imagery for monitoring changes in agricultural land use remains relatively underexplored, particularly within Indonesia's tropical regions.

2. RESEARCH METHOD

2.1. Study Area

West Bandung and Purwakarta Regencies in West Java Province, Indonesia are selected as study area due to their significant agricultural landscapes and notable trends in paddy field conversion; in West Bandung Regency, as of 2016, paddy fields covered approximately 15,953 hectares, with land suitability analyses indicating an availability of 25,147 hectares for potential paddy field development [31], while in Purwakarta Regency, between 2013 and 2017, paddy fields shrank by 195.55 hectares (1%), primarily due to conversions to industrial use (117.99 ha), settlements (42.30 ha), and other infrastructures [32], highlighting the urgent need for research on sustainable rice field management and land use policies.

Our methodology builds upon prior internal research [1], that explored the feasibility of satellite imagery for paddy field mapping. Unlike the earlier study, which provided an initial data assessment without a robust validation framework, this research demonstrates a significant methodological and analytical advancement utilizes Sentinel-1, Sentinel-2, and Landsat-8 imagery from multiple years for a comprehensive spatio-multitemporal analysis.

2.2. Data

This study utilizes medium-resolution optical satellite imagery from Sentinel-1, Sentinel-2, and Landsat-8, with data references from the years 2013 and 2021. Table 1 presents the list of satellite bands employed in this study.

Table 1. List of Sentinel-1, Sentinel-2, and Landsat-8 spectral bands

Name	Spatial Resolution (meters)	Description
Sentinel-1		
HH	10	Single co-polarization, horizontal transmit/horizontal receive
HV	10	Dual-band cross-polarization, horizontal transmit/vertical receive
VV	10	Single co-polarization, vertical transmit/vertical receive
VH	10	Dual-band cross-polarization, vertical transmit/horizontal receive
Sentinel-2		
B1	60	Aerosols
B2	10	Blue
B3	10	Green
B4	10	Red
B5	20	Red Edge 1
B6	20	Red Edge 2
B7	20	Red Edge 3
B8	10	NIR
B8A	20	Red Edge 4
B9	60	Water vapor
B10	60	Cirrus
B11	20	SWIR 1
B12	20	SWIR 2
Landsat-8		
B1	30	Coastal aerosol
B2	30	Blue
B3	30	Green
B4	30	Red
B5	30	Near infrared
B6	30	Shortwave infrared 1
B7	30	Shortwave infrared 2
B8	15	Band 8 Panchromatic
B9	30	Cirrus
B10	30	Thermal infrared 1, resampled from 100m to 30m
B11	30	Thermal infrared 2, resampled from 100m to 30m

The analysis involves the use of several remote sensing indices derived from satellite bands, includes:

1. *Normalized Difference Vegetation Index (NDVI)*

NDVI is used to assess vegetation health and density, calculated using the formula:

$$NDVI = \frac{NIR - Red}{NIR + Red}$$

Higher values generally indicate areas with dense and healthy vegetation cover.

2. *Normalized Difference Water Index (NDWI)*

NDWI highlights water features and moisture in vegetation using the formula:

$$NDWI = \frac{Green - NIR}{Green + NIR}$$

It enhances the visibility of open water and damp surfaces in satellite imagery.

3. *Normalized Difference Built-up Index (NDBI)*

NDBI is designed to identify built-up or urbanized areas and is calculated as:

$$NDBI = \frac{SWIR1 - NIR}{SWIR1 + NIR}$$

This index effectively separates developed land from vegetated or natural areas.

4. *Enhanced Vegetation Index (EVI)*

EVI is optimized for high-biomass regions and reduces atmospheric and canopy background effects. It is computed as:

$$EVI = 2,5 \frac{NIR - Red}{(NIR + 6 Red - 7,5 Blue) + 1}$$

EVI provides more reliable vegetation estimates in densely forested zones.

5. *Soil Adjusted Vegetation Index (SAVI)*

SAVI adjusts vegetation measurements to reduce soil brightness interference, particularly in sparse vegetative areas. The formula is:

$$SAVI = \frac{(NIR - Red)(1 + L)}{NIR + Red + 1}$$

where L is a soil brightness correction factor, often set to 0.5.

6. *Normalized Difference Tillage Index (NDTI)*

NDTI is useful for detecting tillage and land disturbance in agricultural areas. It is calculated using:

$$NDTI = \frac{SWIR1 - SWIR2}{SWIR1 + SWIR2}$$

This index helps differentiate between tilled and untilled soil surfaces.

7. *Bare Soil Index (BSI)*

BSI identifies areas with exposed soil and is calculated with the formula:

$$BSI = 2,5 \frac{[(SWIR1 + Red) - (NIR + Green)]}{[(SWIR1 + Red) + (NIR + Green)]}$$

It effectively separates bare land from vegetated and built-up regions.

2.3. Methods

The research framework for this study integrates remote sensing and deep learning methodologies to address the critical challenges of agricultural land use monitoring, specifically the conversion of paddy fields in Indonesia. Figure 1 illustrates a schematic depiction of the study's research framework. The study acknowledges key limitations of traditional approaches, such as the area sampling frame (ASF) method, which is constrained by cost and accuracy, and the inconsistency in classification accuracy across satellite imagery. Additionally, rapid land use changes and the need for up-to-date rice planting estimates necessitate a more robust and scalable approach. The proposed solution leverages multi-source satellite data, including Sentinel-1, Sentinel-2, and Landsat-8, in combination with advanced machine learning and deep learning techniques. Algorithms such as Random Forest, Support Vector Machines, Decision Trees, and Gradient Boosting, along with deep learning models like Multi-Layer Perceptrons and Convolutional Neural Networks (CNNs), are employed to improve land classification accuracy. The integration of these methodologies ensures a comprehensive, automated, and scalable system for land use change detection.

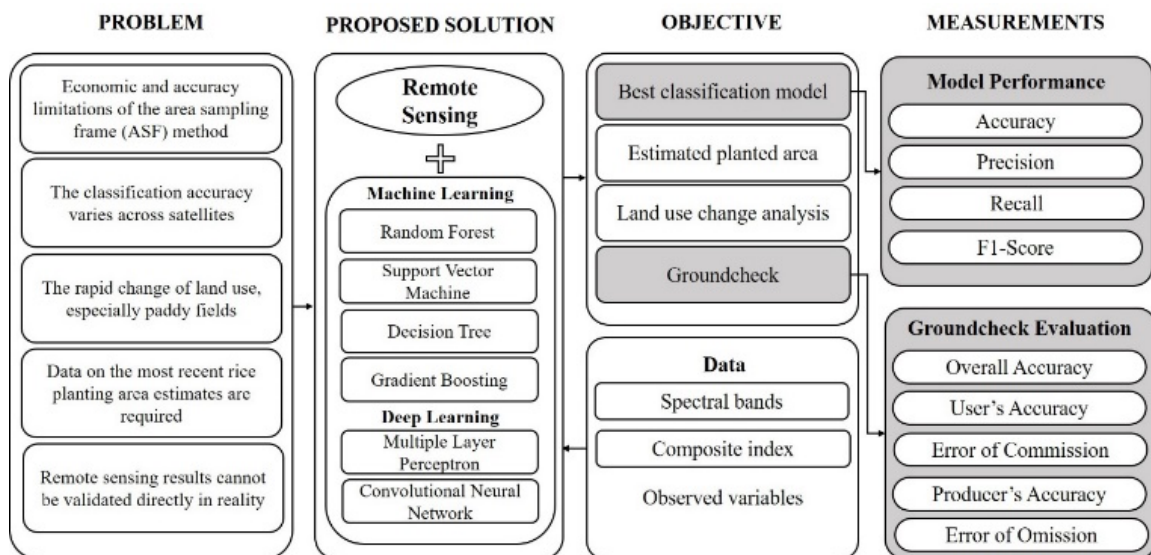


Figure 1. Research framework

The study's objectives are centered on identifying the best classification model for paddy field detection, estimating the planted area, and conducting spatio-multitemporal analyses of land

use conversion. The validation process involves ground-truth evaluations, ensuring that the remote sensing-derived classifications align with real-world observations. Performance metrics such as accuracy, precision, recall, and F1-score are used to assess model effectiveness, while additional ground-check evaluations include overall accuracy, user's accuracy, producer's accuracy, and commission/omission errors. These rigorous assessment measures enhance the reliability of the classification results, offering critical insights into agricultural land dynamics. The findings of this research will aid policymakers in sustainable land management by providing high-resolution, AI-driven insights into the extent and patterns of paddy field loss. Furthermore, the integration of spectral bands, composite indices, and observed variables ensures that the developed model is robust and adaptable to future enhancements in AI-driven land monitoring systems.

2.3.1. Data Acquisition and Preprocessing

To ensure high-quality input data for land cover classification and spatio-multitemporal analysis, this study employs a rigorous data preprocessing pipeline. Preprocessing is a critical step in remote sensing analysis, transforming raw satellite imagery into a structured format suitable for deep learning-based land use classification. The preprocessing workflow consists of three key stages: cloud masking and image patching, feature extraction, and labeling.

2.3.1.1. Cloud masking and image patching

Given the frequent cloud cover in tropical regions, effective cloud removal is essential to preserve the integrity of land cover classification. This study utilizes cloud masking techniques to detect and eliminate clouds and their shadows from Sentinel-1, Sentinel-2, and Landsat-8 imagery. Since cloud occlusion can obscure critical land features, a subsequent image patching process is applied, wherein cloudy pixels are replaced with corresponding cloud-free pixels from temporally adjacent images. The selection of replacement patches is guided by the principles of minimal land cover change and temporal proximity, ensuring the continuity and accuracy of spatial information through a gap-filling approach.

2.3.1.2. Feature Extraction

Following cloud correction, feature extraction is conducted to derive key spectral indices that enhance land cover discrimination. Feature extraction enables the identification of unique geospatial characteristics through mathematical transformations of spectral bands. The features utilized in this land use change mapping study comprise composite indices that represent the geographical characteristics of the study area. Specifically, seven key indices are employed: Normalized Difference Vegetation Index (NDVI), Normalized Difference Water Index (NDWI), Normalized Difference Built-up Index (NDBI), Enhanced Vegetation Index (EVI), Soil Adjusted Vegetation Index (SAVI), Normalized Difference Tillage Index (NDTI), and Bare Soil Index (BSI). These indices collectively improve the model's ability to distinguish between land cover types, ensuring robust classification accuracy.

2.3.1.3. Labeling and sample selection

The final preprocessing step involves labeling, wherein land cover classes are assigned to geospatially homogeneous areas using polygon-based segmentation. This study classifies land cover into six categories: clouds, paddy fields, built-up areas, forests, water bodies, non-vegetative bare land, and fallow land. The labeling process is guided by administrative boundaries, with sample distribution proportional to the fraction of each land cover class within the region. These labeled samples serve as ground truth references, providing a foundation for training and validating the deep learning model. Through this comprehensive preprocessing framework, the study ensures high-fidelity data inputs for deep learning-based agricultural land monitoring, enabling precise detection of paddy field conversion and land use transformation over time.

2.3.2. Modelling

The collected satellite imagery data and corresponding land cover labels serve as the foundation for developing a deep learning-based classification model. This study employs Multilayer Perceptron (MLP) and Convolutional Neural Network (CNN) algorithms, leveraging their proven effectiveness in satellite imagery analysis. Deep learning models are selected due to their superior capacity to capture complex spatial and spectral patterns compared to traditional machine learning approaches. The independent variables in this study comprise composite indices derived from remote sensing data. The manually labeled land cover classes serve as the dependent variable, forming the basis for model training and validation.

A total of twelve classification models are developed, with separate MLP and CNN models trained for West Bandung Regency and Purwakarta Regency, utilizing Landsat-8 (2013 and 2021) and Sentinel-2 (2021) imagery. The models undergo rigorous evaluation using 10-fold cross-validation, ensuring robust performance assessment across multiple iterations. Classification performance is measured using accuracy, precision, recall, and F1-score, providing a comprehensive evaluation of model effectiveness. The highest-performing model is then employed to generate land cover maps, which serve as the basis for subsequent spatio-temporal analysis.

To enhance classification accuracy and reduce noise in the final land cover maps, post-classification processing is conducted. This involves applying a minority/majority filtering technique, which refines classification outputs by reassigning ambiguous pixels based on the dominant surrounding land cover class. This approach ensures greater spatial coherence and minimizes classification errors. The final land cover maps are then subjected to both quantitative and visual evaluation, ensuring their reliability for further analysis. The best-performing results are subsequently utilized to assess land use conversion trends and inform policy recommendations for sustainable land management.

2.3.3. Ground truth check

Ground truth verification is a critical step in validating satellite imagery-based classification by comparing the spectral and spatial characteristics of objects in remote sensing data with their real-world counterparts. In this study, ground verification was conducted during fieldwork activities from January 31 to February 6, 2022. The classification results were systematically evaluated using a confusion matrix, a widely adopted method for assessing classification accuracy by quantifying agreement between predicted and actual land cover classes.

Given constraints related to cost, time, and manpower, ground truth data collection was conducted in selected areas using a stratified random sampling approach. This approach entails stratifying the study area according to distinct land cover categories, followed by the random selection of sampling points within each defined stratum. Stratification ensures balanced representation across land cover types, reducing bias and improving the robustness of accuracy assessment. According to Haub (2015), stratification can be based on factors such as land cover, agroecological zones, map complexity, elevation, trends, administrative units, or other relevant attributes that influence spatial variability. By stratifying based on land cover class, this study ensures an adequate and proportional distribution of sample points across different land categories, enhancing the reliability of classification validation. Once the strata were established, simple random sampling was applied to select specific validation points within each stratum. The scope of this study, including details of the sampling strategy and validation approach, is further elaborated in Table 2.

Table 2. Scope of The Study

Scope	Description
Population	All land cover in West Bandung Regency and Purwakarta Regency, both in West Java Province Indonesia, between 2013 and 2021
Target population	<ol style="list-style-type: none"> 1. Paddy fields designated for food crops consisting of wetland agricultural land, dry land agricultural land, and fallow. 2. Built-up areas includes buildings, houses, closed infrastructure, offices, toll roads, cross-provincial and district/city roads, and other roads that are quite wide 3. Forest contains shrubs, grasslands, trees, tree-based plantations, and all types of forests.

Deep Learning and Remote Sensing for Agricultural Land Use Monitoring... (Ari Wahyu Wijayanto)

Scope	Description
Observation unit	4. Water.
	5. Non-vegetative bare land including ex-mining and open land.
Analysis unit	Classified land cover points
Sampling frame	<ol style="list-style-type: none"> 1. Land cover map of West Bandung Regency and Purwakarta Regency, West Java Province Indonesia, in 2013 and 2021. 2. Medium resolution optical satellite images of Sentinel-1, Sentinel-2, and Landsat-8 for the West Bandung Regency and Purwakarta Regency areas. 3. The sample framework used for ground checking is the 2021 land cover map from modeling results using Sentinel-2 medium resolution optical imagery.

2.3.4. Analysis

2.3.4.1. Rice planting area calculation

The estimation of rice planting area was carried out based on the mapping results of land cover classification using Sentinel-2 and Landsat-8 imagery. To determine the projected rice planting area, it is assumed that all land that has been categorized as paddy fields is planted with rice.

$$\text{rice planting area} = \text{number of pixels} \times \text{area per pixel}$$

The area of each pixel can be seen from the spatial resolution (Cahyono et al., 2019). The Sentinel-2 image has a spatial resolution of 10 m x 10 m and a pixel area of 100 m². Meanwhile, Landsat-8 imagery with a spatial resolution of 30 m x 30 m has an area of 900 m² per pixel.

2.3.4.2. Land cover conversion analysis

Detection of land that changes function is employed using the Post-Classification Change Detection (PCCD) approach. PCCD is a technique that produces land change maps based on the overlay of two maps of different years.

$$V = \frac{A_{2021} - A_{2013}}{A_{2013}} \times 100\%$$

With V (change in land use (%)), A_{2021} (land area in 2021 (ha)), A_{2013} (land area in 2013 (ha)).

This technique is based on the comparison of pixels from two images. First, overlaying two classified maps from Landsat-8 satellite imagery in 2013 and 2021. Then compare the pixels on the 2013 and 2021 maps to find out changes in land cover that have occurred. The size of each pixel can be seen from the image resolution used, which is 30 m x 30 m or 900 m².

2.3.4.3. Paddy field land use conversion rate analysis

Land use change refers to the transformation of land from one designated use to another, often driven by socio-economic, environmental, and policy factors. In the context of this study, land conversion specifically pertains to the transformation of agricultural land, particularly paddy fields, into non-agricultural land uses. This shift may occur either permanently or temporarily, leading to the loss of productive rice-growing areas. The study focuses on the conversion of paddy fields into non-rice fields, which are categorized as built-up areas, forests, water bodies, and non-vegetative bare land.

To quantify the extent of this transition, the land conversion rate is defined as a metric representing the average rate at which paddy fields are converted into non-rice fields over a specified time period. This rate serves as a critical indicator for assessing the magnitude and pace of agricultural land loss, which has significant implications for food security, environmental sustainability, and regional land use planning. The calculation of land conversion is conducted using Formula X, which provides a standardized approach for measuring and analyzing these changes.

$$X_i = \frac{n_i}{N_i} \times 100\%$$

where

X_i : Land conversion rate in the i-th sub-district

n_i : Number of pixels of interest classified as non-rice fields in 2021 in the i-th sub-district

N_i : Number of pixels of interest classified as rice fields in 2013 in the i-th sub-district

Pixels of interest are pixels that are not classified as clouds in 2013 or 2021.

Land conversion analysis is carried out partially and continuously. Partial analysis is used to determine the rate of rice field conversion from year to year, while continuous analysis is used to determine the growth rate of land area over a certain period of time. To calculate the rate of land conversion, the following formula can be used.

$$V = \frac{L_t - L_{t-1}}{L_{t-1}} \times 100\%$$

where

V : Land conversion rate (%)

L_t : Land area in year t (ha)

L_{t-1} : Land area in year before t (ha)

The rate of land conversion is calculated by comparing the land area in year t to that of the preceding year. Specifically, it is determined by subtracting the land area in the previous year from the area in year t, dividing the result by the previous year's land area, and then multiplying by 100 to express it as a percentage. This method can be applied iteratively for each year to derive annual land conversion rates over a given period. If the V value of a land cover is less than zero, then the area of the land cover is interpreted as having decreased. The calculation results obtained are entered in the following land cover change rate tabulation table.

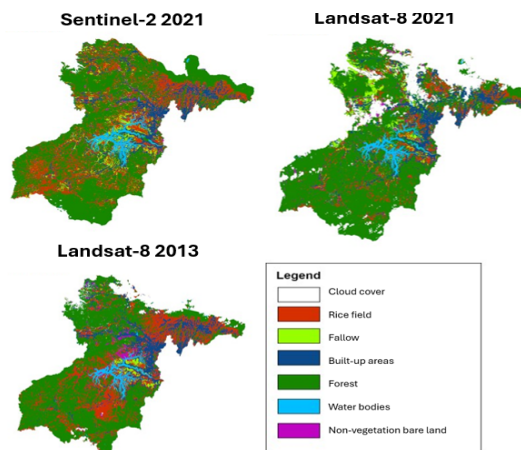


Figure 2. Comparison of land cover classification data from the Sentinel-2 2021 (a) and Landsat-8 2021 (b) satellites in West Bandung Regency

For each regency, the developed model is then used to predict land cover. Figure 2 depicts a comparison of land cover classification data from the Sentinel-2 2021 (a) and Landsat-8 2021 (b) satellites in West Bandung Regency. The findings show that cloud cover is predominantly detected in the Landsat-8 satellite classification results since the acquired Landsat-8 imagery has a lot of cloud cover. This demonstrates that in West Bandung Regency 2021, Landsat-8 remote sensing satellite imagery is more sensitive to cloud cover than Sentinel-2. A comparison of the classification results of the Sentinel-2 2021 (a) and Landsat-8 2013 (b) satellites shows that the two have a similar pattern. Built-up areas, forests, and non-vegetative bare land were all narrowed in 2021. Otherwise, rice fields and water bodies have expanded.

3. RESULTS AND DISCUSSION

3.1. Model Development Results

Table 3 summarizes the results of the developed model's evaluation. It shows that the built model is good enough with accuracy, precision, recall, and an F1-score of more than 0.7. In addition, the

convolutional neural networks (CNN) model outperforms the multilayer perceptron (MLP) model, and the use Sentinel-2 remote sensing satellite image gives competitive advantage than Landsat-8.

Table 3. Modeling Results

Evaluation	Model	Sentinel-2 2021 (West Bandung)	Landsat-8 2021 (West Bandung)	Landsat-8 2013 (West Bandung)	Sentinel-2 2021 (Purwakarta)	Landsat-8 2021 (Purwakarta)	Landsat-8 2013 (Purwakarta)
Accuracy	MLP	0.92	0.78	0.93	0.9	0.77	0.78
	CNN	0.96	0.89	0.93	0.93	0.9	0.88
Precision	MLP	0.92	0.78	0.93	0.9	0.77	0.78
	CNN	0.96	0.89	0.93	0.93	0.9	0.88
Recall	MLP	0.8	0.64	0.91	0.84	0.63	0.65
	CNN	0.95	0.85	0.9	0.91	0.84	0.81
F1-Score	MLP	0.82	0.68	0.92	0.87	0.69	0.7
	CNN	0.95	0.87	0.92	0.92	0.87	0.84

Figure 3 depicts a comparison of land cover classification data from the Sentinel-2 2021 (a) and Landsat-8 2021 (b) satellites in Purwakarta Regency. A comparison of the classification results of the Sentinel-2 2021 (a) and Landsat-8 2013 (b) satellites shows that the two have a similar pattern. Water bodies and non-vegetative bare land were narrowed in 2021. Otherwise, rice fields and built-up areas have expanded.

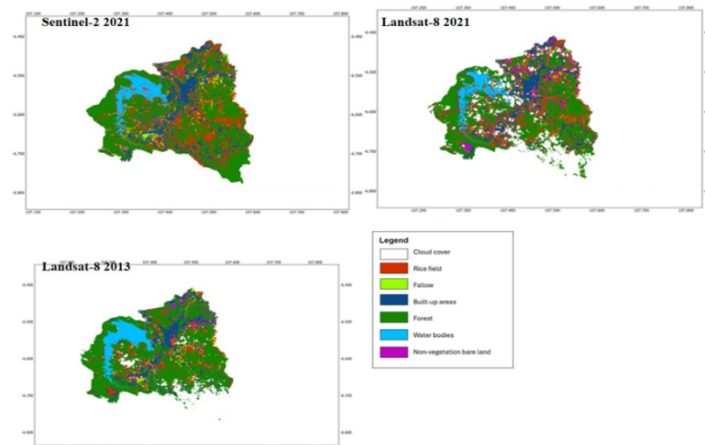


Figure 3. Comparison of land cover classification data from the Sentinel-2 2021 (a) and Landsat-8 2021 (b) Satellites in Purwakarta Regency

3.2. Ground Truth Evaluation

The evaluation (in proportion) of the ground truth check findings in this study is shown in Table 4. In this study, a ground truth check was carried out to validate the estimated land cover based on Sentinel-2 remote sensing satellite imagery in 2021. The calculation results show that the total accuracy value is 78.22 percent, which implies that the land cover that is accurately classified is 78.22 percent. The forest class had the highest user and producer accuracy, with 90.03 percent and 83.92 percent, respectively. Meanwhile, the lowest user's accuracy and producer's accuracy values were in the non-vegetative bare land class, respectively at 35.09 percent and 41.50 percent. In contrast, the error of commission and error of omission values where the highest values of the two values occur in the non-vegetative bare land class are respectively 64.91 percent and 58.50 percent.

Meanwhile, the lowest error of commission and error of omission values of the two values occurred in the forest class respectively at 9.97 percent and 16.08 percent.

Table 4. Ground truth results coefficient matrix

Remote sensing results	Ground truth results					Total	User's accuracy	Error of commission
	Rice field	Built-up area	Forest	Water bodies	Non-vegetative bare land			
Rice field	0.2188	0.0191	0.051	0.004	0.0098	0.3027	0.7229	0.2771
Built-up area	0.0138	0.0733	0.0252	0.0013	0.0013	0.115	0.6374	0.3626
Forest	0.0416	0.003	0.4562	0.0015	0.0045	0.5067	0.9003	0.0997
Water bodies	0.0069	0.0013	0.0084	0.0215	0.002	0.0401	0.5351	0.4649
Non-vegetative bare land	0.0124	0.0078	0.0027	0.0002	0.0125	0.0355	0.3509	0.6491
Total	0.2935	0.1044	0.5436	0.0285	0.03	1		
Producer's accuracy	0.7456	0.7019	0.8392	0.7531	0.415	Overall accuracy		0.7822
Error of omission	0.2544	0.2981	0.1608	0.2469	0.585			

3.3. Land Cover Conversion Analysis

Table 5. Changes in West Bandung Regency and Purwakarta Regency land cover

Land cover type	West Bandung						Purwakarta					
	2013		2021		Changes		2013		2021		Changes	
	Area (ha)	%	Area (ha)	%	Area (ha)	%	Area (ha)	%	Area (ha)	%	Area (ha)	%
Paddy field	29,714.04	25.05	18,401.49	16.42	11,312.5	-38.07	12,926.88	14.81	18,287.55	21.48	5,360.67	41.47
Built-up area	15,796.17	13.32	13,488.48	12.03	2,307.69	-14.61	10,808.46	12.38	11,948.13	14.04	1,139.67	10.54
Forest	67,356.81	56.78	75,170.25	67.06	7,813.44	11.60	53,127.27	60.85	44,610.21	52.41	8,517.06	-16.03
Water bodies	3,957.48	3.34	3,675.87	3.28	281.61	-7.12	7,858.44	9.00	5,012.91	5.89	2,845.53	-36.1
Non-vegetative bare land	1,797.84	1.52	1,363.05	1.22	434.79	-24.18	2,591.64	2.96	1,363.05	6.18	2,676.87	103.61
Total	118,622.34	100.00	112,099.10	100.00	22,150.00		87,312.69	100.00	83,520.09	100		

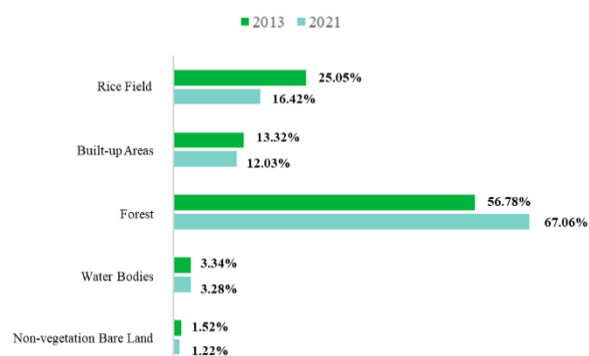


Figure 4. Comparison of land cover proportion in West Bandung Regency between 2013 and 2021

Figure 4 shows that the four categories of land cover (built-up areas, paddy fields, non-vegetative bare land, and water bodies) have decreased. This signifies that the land area in 2013 is greater than 2021. Built-up area decreased by 14.61 percent. Likewise, paddy fields decreased by

38.07 percent, non-vegetative bare land decreased by 24.18 percent, water bodies decreased by 7.12 percent. On the other hand, forests increased by 11.60 percent. In West Bandung Regency, the change in paddy fields reached 38.07 percent between 2013 and 2021, which is the greatest change, implying that it changed by 4.76 percent per year. Water bodies witnessed the least change, with a change of 7.12 percent in land cover. Figure 5 depicts a thematic map of the percentage of yearly rice field changes for each subdistrict in West Bandung Regency.

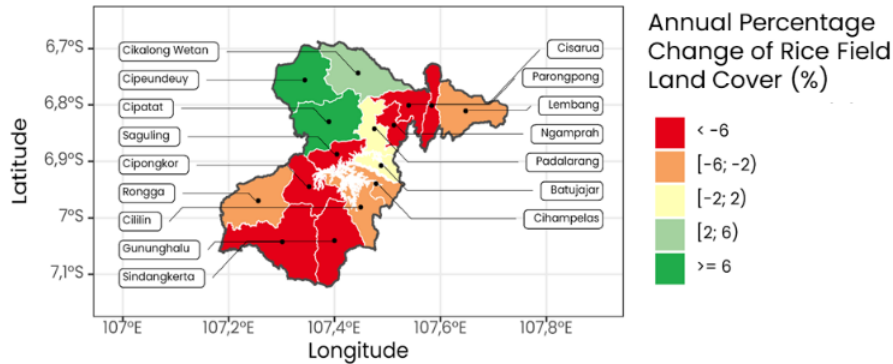


Figure 5. Yearly sub district level paddy field land cover changes in West Bandung Regency in percentage

Based on Figure 5, the majority of the sub-districts witnessed an annual change in paddy field land cover of more than 6%, either in increase or decrease. Cisarua, Parangpong, Ngamprah, Saguling, Cipongkor, Gununghalu, and Sindangkerta Districts had decrease of less than 6%. Cipeundeuy and Cipatat Districts were among those that witnessed increase. Padalarang and Batujajar Subdistricts have a relatively small proportion of land cover change, with an annual paddy field cover change of less than 2%. Statistics from the Food Crops and Horticulture Service on the area of paddy field area per regency in West Java for 2013-2020 show a change in paddy field area of 5,069 hectares with a percentage change of 1.73 percent. This comparison yielded a relative error value of 6.49 percent.

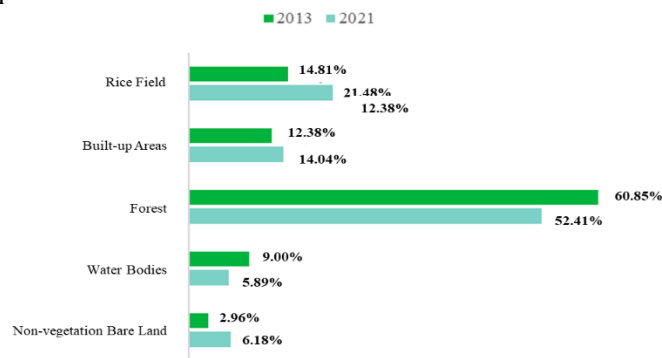


Figure 6. Comparison of land cover proportion in Purwakarta Regency between 2013 and 2021

Figure 6 shows that the three categories of land cover (paddy fields, built-up area, and non- vegetative bare land) have increased. This indicates that the land area in 2013 is smaller than 2021. On the other hand, forests and water bodies have decreased. The biggest change occurred in non-vegetative bare land which increased by 103.61%, from 2.96% to 6.18%. Built-up areas witnessed the least change, with a 10.54% increased change in land cover area. Paddy fields increased by 41.47%. The forest decreased by 16.03%, and water bodies decreased by 36.21%. The area of paddy fields in Purwakarta Regency has changed by 41.47 percent in eight years, or 5.18 percent each year. Figure 7 thematic maps show details on the percentage change for each sub-district.

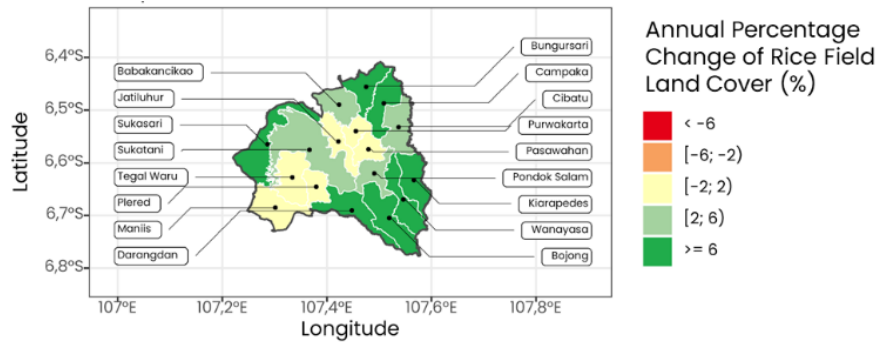


Figure 7. Yearly sub district level paddy field land cover change in Purwakarta Regency in percentage

Based on Figure 7, it can be seen that the most sub-districts had an increase in annual paddy field cover of more over 6%, including Bungursari, Campaka, Sukasari, Kiarapedes, Wanayasa, Bojong, and Darangdan. However, Cibatu, Pasawahan, Jatiluhur, Tegal Waru, Plered, and Maniis are sub-districts that have a relatively small percentage of land cover change, which is less than 2%. Statistics Indonesia (Purwakarta Regency) shows that the area of paddy fields in 2013 was 16,573 ha and 17,907 ha in 2021 with a percentage change of 1.01 percent (1,334 ha). This comparison yielded a relative error value of 4.18 percent. Moreover, Statistics from the Food Crops and Horticulture Service on the area of paddy field area per regency in West Java for 2013-2020 show a change in paddy field area of 5,069 hectares with a percentage change of 1.73 percent. This comparison yielded a relative error value of 6.49 percent. Moreover, a relative error score of 4.58 percent was obtained when comparing data from the Food Crops and Horticulture Service in terms of rice planting area per regency in West Java from 2013 to 2020.

3.4. Estimating Rice Planting Area

Land area calculation was generated using the Sentinel-2 satellite's land cover data to determine the rice planting area in West Bandung and Purwakarta Regencies in 2021. Table 6 displays the land area estimation results.

Table 6. Estimated paddy field area

Land cover classification	West Bandung 2021 land cover area		Purwakarta 2021 land cover area	
	ha	%	ha	%
Built-up area	13.796.24	11.00	14.268.91	14.35
Paddy field	39.968.56	31.90	25.377.16	25.52
Forest	69.607.37	55.55	52.164.11	52.46
Non-vegetative dry land	784.51	0.63	1.529.49	1.54
Water bodies	1.149.73	0.92	6.094.43	6.13
Total	125.306.40	100.00	99.434.10	100.00

The number of pixels for each classification of land cover is calculated from the labeling results and then transformed into a unit area. According to the table of land cover results in 2021 for West Bandung Regency, the land cover area for the paddy field type was 39,968.55 ha (31.90%), while the land cover area for Purwakarta Regency was 25,377.16 ha (25.50%). Generally, the estimated paddy area in West Bandung Regency is 6.40 percent larger than in Purwakarta Regency.

Figure 8 shows the total area of paddy fields in West Bandung Regency at the sub-district level. Of the 16 sub-districts in West Bandung Regency, Gununghalu subdistrict has the highest rice planting area of 4,911.88 ha because many farmers were opening new paddy field areas in that region. In contrast, the lowest rice planting area was Parongpong subdistrict with 961.64 ha rice planting area due to land use changes that occur suddenly in a short period of time.

The overall predicted rice planting area for 2021 in West Bandung Regency is 39,968.55 ha, whereas the total area for comparative data received from the Food Crops and Horticulture Department for 2020 is 45,713 ha. Based on this comparison, the relative inaccuracy is 12.56 percent.

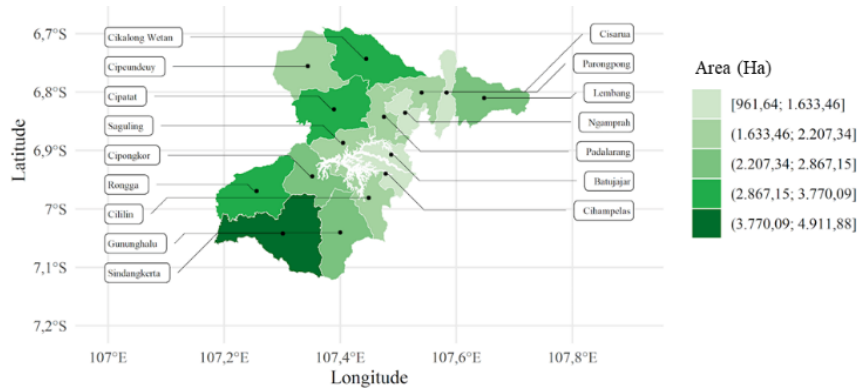


Figure 8. Visualization of subdistrict level estimated rice planting area of West Bandung Regency in 2021

Figure 9 shows the total rice planting area (ha) for each sub-district in Purwakarta Regency in 2021 obtained from the calculation results based on Sentinel-2 satellite imagery. Of the 17 sub-districts in Purwakarta Regency, Sukatani subdistrict has the highest rice planting area of 2,781.48 ha because many farmers were opening new paddy field areas in that region. In contrast, the lowest rice planting area was Parongpong subdistrict with 434.96 ha rice planting area due to land use changes that occur suddenly in a short period of time. The overall predicted rice planting area for 2022 in Purwakarta Regency is 25,377.16 ha, whereas the total area for comparative data received from the Statistics Indonesia for 2020 is 24.270 ha. Based on this comparison, the relative inaccuracy is 4.56 percent.

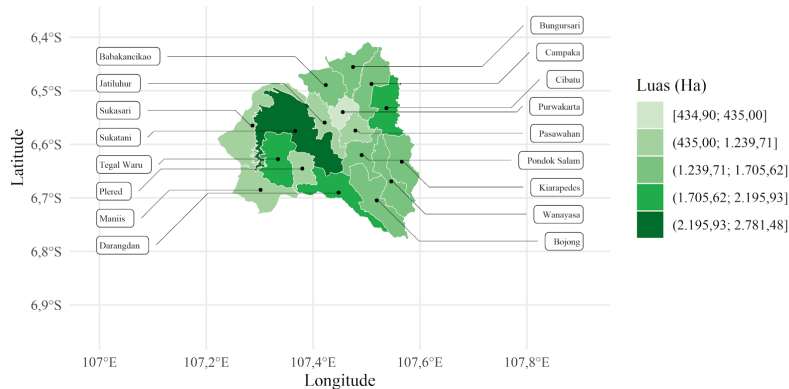


Figure 9. Visualization of subdistrict level estimated rice planting area of Purwakarta Regency in 2021

3.5. Paddy Field Land Use Conversion Rate

Figure 10 illustrates the rate of land-use changes in West Bandung Regency by sub-district. It can be seen that the subdistrict with the greatest rate of paddy fields change in West Bandung Regency is Saguling, which is equivalent to 76.35%. However, the sub-district with the lowest percentage of paddy field change was Cikalong Wetan Subdistrict, at 38.66%. The average land use change in West Bandung Regency is fairly large, which is 56.75%. Cililin, Cipongkor, Gununghalu, Ngamprah, Rongga, Saguling, and Sindangkerta are seven of the 16 sub-districts of West Bandung Regency that have higher rates of land conversion than the average. Meanwhile, nine other sub-districts that have below average rates of land conversion include Batujajar,

Cihampelas, Cikalong Wetan, Cipatat, Cipeundeuy, Cisarua, Lembang, Padalarang, and Parongpong.

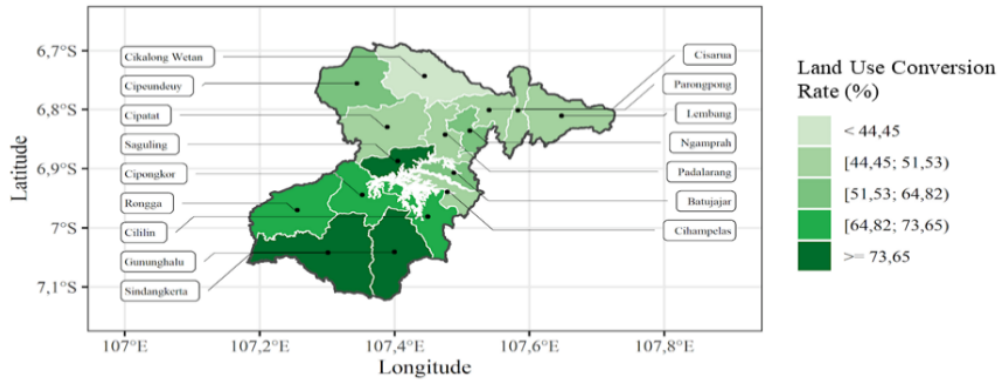


Figure 10. Thematic map of land change rates in West Bandung Regency

Figure 11 illustrates the rate of land-use changes in Purwakarta Regency by sub-district. It can be seen that the subdistrict with the greatest rate of paddy fields change in Purwakarta Regency is Maniis, which is equivalent to 63.38%. However, the sub-district with the lowest percentage of paddy field change was Bojong Subdistrict, at 19.84%. The average land use change in West Bandung Regency is 32.94%. Jatiluhur, Sukasari, Maniis, Sukatani, Pasawahan, Purwakarta, dan Sindangkerta are seven of the 17 sub-districts of West Bandung Regency that have higher rates of land conversion than the average. Meanwhile, ten other sub-districts that have below average rates of land conversion include Bungursari, Cibatu, Campaka, Pondok Salam, Kiarapedes, Wanayasa, Bojong, Darangdan, Plered, dan Tegal Waru.

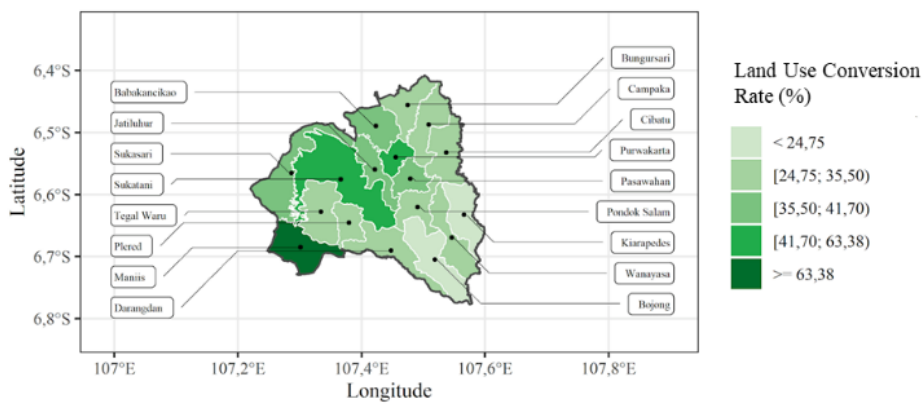


Figure 11. Land use conversion rates in Purwakarta Regency

3.6. Discussion

Table 11 shows the matrix of changes in land cover area (ha) in West Bandung Regency. It can be seen that the largest land cover that has not changed from 2013 to 2021 is forest with an area of 51,756.21 ha, while the smallest is vacant non-vegetative land with an area of 215.10 ha. Paddy fields covered 27,154.98 hectares in 2013, but by 2021, the area had decreased to 17,734.23 ha, with 9,585.54 ha remaining unchanged since 2013. The change in paddy field area consisted of 1,933.47 ha which turned into built-up areas, 15,125.76 ha into forest, 169.29 ha into water bodies, and 340.92 ha into non-vegetative bare land. In 2021, the built-up areas area has decreased from 14,966.37 hectares in 2013 to 13,090.23 ha. The decrease in area was caused by changes in the area of paddy fields by 2,083.95 ha, forests by 3,062.07 ha, water bodies by 31.95 ha, non-vegetative bare land by 136.44 ha, and the remainder still being built-up areas by 9,651.96 ha. The forest area has increased from 59,044.95 ha to 71,029.89 ha. The increase in forest area

was caused by changes in other land cover including paddy fields, built-up areas, water bodies, and non-vegetative bare land which turned into forest. However, the area of water bodies has decreased from 3,799.89 hectares in 2013 to 3,603.42 ha in 2021. Non-vegetative bare land decreased to 1,187.55 hectares in 2021.

Table 11. Land cover area changes in West Bandung Regency

2013 → 2021	Rice Fields	Built-up	Forest	Water	Non-vegetative	Total
Rice Fields	9585.54	1933.47	15125.76	169.29	340.92	27154.98
Built-up Land	2083.95	9651.96	3062.07	31.95	136.44	14966.37
Forest	5389.74	1301.49	51756.21	122.22	475.29	59044.95
Water Bodies	111.33	21.78	401.76	3245.22	19.8	3799.89
Non-vegetated Bare Land	563.67	181.53	684.09	34.74	215.1	1679.13
Total	17734.23	13090.23	71029.89	3603.42	1187.55	106645.3

Table 12. Land cover area changes in Purwakarta Regency

2013 → 2021	Rice Fields	Built-up	Forest	Water	Non-vegetative	Total
Rice Fields	7549.74	609.84	1831.5	148.68	1729.53	11869.29
Built-up Land	1259.19	7375.68	539.73	18.09	569.25	9761.94
Forest	6459.75	2626.83	36855.27	52.47	1811.25	47805.57
Water Bodies	743.04	520.65	832.68	4752.54	345.15	7194.06
Non-vegetated Bare Land	1148.94	245.79	299.88	27.72	635.4	2357.73
Total	17160.66	11378.79	40359.06	4999.5	5090.58	78988.59

Table 12 shows the matrix of changes in land cover area (ha) in Purwakarta Regency. Based on Table 12, it can be seen that in 2021 the area of paddy fields in the Purwakarta Regency was 17,160.66 ha, greater than in 2013 (11,869.66 ha). Built-up areas has also increased in area. In 2013, the built-up area was 9,761 ha; in 2021 the area changed to 11,378.79 ha. In contrast to paddy fields and built-up areas, forests and water bodies are decreasing in size. In 2013, forest area and water body area were 47,805.57 ha and 7,194.06 ha respectively. However, in 2021 forests and water bodies have changed respectively to 40,359.06 ha and 4,999.50 ha.

Purwakarta Regency's built-up areas witnessed less change in land area than West Bandung Regency. In contrast, the other four categories of land cover in Purwakarta Regency, including as paddy fields, forest, non-vegetative bare land, and water bodies, had a greater change in land area than West Bandung Regency. As a result, the majority of land cover changes happened in Purwakarta Regency.

According to the rate of paddy field conversion, West Bandung Regency has a substantially higher rate of land conversion than Purwakarta Regency; the average rate of land conversion in West Bandung Regency is 56.75%, while the rate in Purwakarta Regency is 32.94%. Moreover, West Bandung Regency has nine sub-districts with a land conversion rate greater than 50%, but Purwakarta Regency has just one sub-district. This demonstrates that not many inhabitants in Purwakarta Regency have transformed the function of paddy fields to non-rice fields, which is inversely proportional to West Bandung Regency, where many people have converted the function of paddy fields to non-rice fields. The value of changes in land conversion also shows that there is a reduction in land conversion in paddy fields in West Bandung Regency. Neural Network (CNN) model outperforms the Multilayer Perceptron (MLP) model in classifying land cover, and that Sentinel-2 imagery provides higher classification accuracy compared to Landsat-8. The evaluation metrics reveal a high overall classification accuracy, with 78.22% of land cover correctly classified, underscoring the reliability of deep learning models in remote sensing applications.

A comparative analysis of land cover changes between 2013 and 2021 reveals significant regional variations. Built-up areas in Purwakarta Regency exhibited less expansion than in West Bandung Regency. However, other land cover types in Purwakarta Regency, including paddy fields, forests, non-vegetative bare land, and water bodies, underwent more substantial changes

compared to West Bandung Regency. The findings suggest that West Bandung Regency has a higher overall rate of land use change, yet the conversion of land to paddy fields has been declining. Notably, forests are the only land cover category in West Bandung Regency that has increased in area since 2013. In contrast, Purwakarta Regency experienced an increase in both paddy field and built-up area extents, while forests and water bodies showed relatively smaller changes.

These findings highlight the potential of integrating deep learning and remote sensing for large-scale agricultural land monitoring, offering a cost-effective and scalable approach for tracking land use changes and informing sustainable land management policies. Future research should explore higher-resolution satellite imagery and more advanced deep learning architectures to further enhance classification accuracy and predictive capabilities.

4. CONCLUSION

This study demonstrates the effectiveness of medium-resolution optical satellite imageries, specifically Sentinel-1, Landsat-8, and Sentinel-2, in mapping and analyzing the classification and conversion of agricultural land. The results indicate that the Convolutional Neural Network (CNN) model outperforms the Multilayer Perceptron (MLP) model in classifying land cover, and that Sentinel-2 imagery provides higher classification accuracy compared to Landsat-8. The evaluation metrics reveal a high overall classification accuracy, with 78.22% of land cover correctly classified, underscoring the reliability of deep learning models in remote sensing applications.

A comparative analysis of land cover changes between 2013 and 2021 reveals significant regional variations. Built-up areas in Purwakarta Regency exhibited less expansion than in West Bandung Regency. However, other land cover types in Purwakarta Regency, including paddy fields, forests, non-vegetative bare land, and water bodies, underwent more substantial changes compared to West Bandung Regency. The findings suggest that West Bandung Regency has a higher overall rate of land use change, yet the conversion of land to paddy fields has been declining. Notably, forests are the only land cover category in West Bandung Regency that has increased in area since 2013. In contrast, Purwakarta Regency experienced an increase in both paddy field and built-up area extents, while forests and water bodies showed relatively smaller changes.

Our findings highlight the potential of integrating deep learning and remote sensing for large-scale agricultural land monitoring, offering a cost-effective and scalable approach for tracking land use changes and informing sustainable land management policies. Future research should explore higher-resolution satellite imagery and more advanced deep learning architectures to further enhance classification accuracy and predictive capabilities.

REFERENCES

- [1] M. A. Elbehri, A. Kaminski, and D. Dawe, "The changing structure of the world rice market, 2000–2015," *Food Policy*, vol. 92, p. 101832, 2020.
- [2] J. Fanzo, C. Davis, R. McLaren, and J. Choufani, "The effect of climate change across food systems: Implications for nutrition outcomes," *Global Food Security*, vol. 18, pp. 12–19, 2018.
- [3] U.S. Department of Agriculture, Foreign Agricultural Service, "Indonesia Rice Area, Yield and Production," [Online]. Available: <https://ipad.fas.usda.gov/countrysummary/Default.aspx?crop=Rice&id=ID>. [Accessed: Mar. 10, 2025].
- [4] A. R. Jensen, *Introductory Digital Image Processing: A Remote Sensing Perspective*, 4th ed. Upper Saddle River, NJ, USA: Prentice Hall, 2015.
- [5] S. Sefrin, M. Schmitt, and X. X. Zhu, "Detection of Land Use and Land Cover Changes Using Sentinel-2 Data: A Case Study of Klingenberg, Saxony, Germany," in *Proc. IEEE Int. Geosci. Remote Sens. Symp. (IGARSS)*, 2020, pp. 1234–1237.
- [6] S. Wang, X. Liu, and Y. Zhou, "Remote Sensing-Based Detection and Prediction of Land Use and Land Cover Changes in Nepal," *Remote Sens.*, vol. 12, no. 5, pp. 1–19, 2020.

- [7] M. Hussain, S. Chen, and A. Cheng, "Remote Sensing-Based Analysis of Land Use/Land Cover Changes and Their Impact on Land Surface Temperature: A Case Study of Khanewal District, Punjab, Pakistan," *Sustainability*, vol. 13, no. 5, pp. 1–17, 2021.
- [8] BPS, "Weekly Average Consumption of Several Food Items Commodity per Capita, 2007–2024," [Online]. Available: <https://www.bps.go.id/en/statistics-table/1/OTUwIzE%3D/weekly-average-consumption-of-several-food-items-commodity-per-capita--2007-2023.html>. [Accessed: Mar. 10, 2025]
- [9] U.S. Department of Agriculture, Foreign Agricultural Service, "Production: Commodity: Rice," [Online]. Available: <https://www.fas.usda.gov/data/production/commodity/0422110>. [Accessed: Mar. 10, 2025].
- [10] BPS, "Harvest Area and Rice Production in Jawa Barat Province 2023," Sep. 2024. [Online]. Available: <https://jabar.bps.go.id/en/publication/2024/09/17/aee55363c1293f361932247a/harvest-area-and-rice-production-in-jawa-barat-province-2023.html>. [Accessed: Mar. 10, 2025].
- [11] A. W. Wijayanto, D. W. Triscowati, and A. H. Marsuhandi, "Maize field area detection in East Java, Indonesia: An integrated multispectral remote sensing and machine learning approach," in *Proc. 2020 12th Int. Conf. Inf. Technol. Electr. Eng. (ICITEE)*, 2020.
- [12] R. Kurniawan, A. M. W. Saputra, A. W. Wijayanto, and W. Caesarendra, "Eco-environment vulnerability assessment using remote sensing approach in East Kalimantan, Indonesia," *Remote Sens. Appl.: Soc. Environ.*, vol. 27, p. 100791, 2022.
- [13] A. W. Wijayanto, N. Afira, and W. Nurkarim, "Machine learning approaches using satellite data for oil palm area detection in Pekanbaru City, Riau," in *Proc. 2022 IEEE Int. Conf. Cybern. Comput. Intell. (CyberneticsCom)*, 2022.
- [14] K. Aprianto, A. W. Wijayanto, and S. Pramana, "Deep learning approach using satellite imagery data for poverty analysis in Banten, Indonesia," in *Proc. 2022 IEEE Int. Conf. Cybern. Comput. Intell. (CyberneticsCom)*, 2022.
- [15] A. W. Wijayanto and S. R. Putri, "Estimating rice production using machine learning models on multitemporal Landsat-8 satellite images (Case Study: Ngawi Regency, East Java, Indonesia)," in *Proc. 2022 IEEE Int. Conf. Cybern. Comput. Intell. (CyberneticsCom)*, 2022.
- [16] W. Nurkarim and A. W. Wijayanto, "Building footprint extraction and counting on very high-resolution satellite imagery using object detection deep learning framework," *Earth Sci. Inform.*, 2023.
- [17] S. R. Putri, A. W. Wijayanto, and S. Pramana, "Multi-source satellite imagery and point of interest data for poverty mapping in East Java, Indonesia: Machine learning and deep learning approaches," *Remote Sens. Appl.: Soc. Environ.*, vol. 29, p. 100889, 2023.
- [18] B. V. R. Zalukhu, A. W. Wijayanto, and M. I. Habibie, "Marine vessels detection on very high-resolution remote sensing optical satellites using object-based deep learning," in *Proc. 2022 IEEE Int. Conf. Commun., Netw. Satellite (COMNETSAT)*, pp. 149–154, 2022.
- [19] N. A. Utami, A. W. Wijayanto, S. Pramana, and E. T. Astuti, "Spatially granular poverty index (SGPI) for urban poverty mapping in Jakarta metropolitan area (JMA): A remote sensing satellite imageries and geospatial big data approach," *Earth Sci. Inform.*, vol. 16, pp. 3531–3544, 2023.
- [20] M. S. C. Claire, S. R. Putri, and A. W. Wijayanto, "A land cover change analysis of buffer areas in New Capital City of Nusantara, Indonesia: A cellular automata approach on satellite imageries data," in *Proc. Int. Conf. Data Sci. Official Stat.*, vol. 2023, no. 1, pp. 132–149, 2023.
- [21] N. A. Daulay, S. R. Putri, A. W. Wijayanto, and I. Y. Wulansari, "Optimizing malaria control: Granular and cost-effective mosquito habitat index in endemic areas through satellite imagery," *Knowl. Eng. Data Sci.*, vol. 7, no. 1, pp. 40–57, 2024.
- [22] M. Feriyanto, A. W. Wijayanto, I. Y. Wulansari, and N. B. Parwanto, "Small area estimation approaches using satellite imageries auxiliary data for estimating per capita expenditure in West Java, Indonesia," *J. Apl. Stat. Komput. Stat.*, vol. 16, no. 2, 2024.

- [23] M. Forkel, N. Carvalhais, C. Rödenbeck, M. D. Mahecha, K. Thonicke, and M. Reichstein, "Trend change detection in NDVI time series: Effects of inter-annual variability and methodology," *Remote Sensing*, vol. 5, no. 5, pp. 2113-2144, 2013.
- [24] S. Du, Y. Zhang, F. Ling, Y. Wang, and W. Li, "Water bodies' mapping from Sentinel-2 imagery with modified normalized difference water index at 10-m spatial resolution produced by sharpening the SWIR band," *Remote Sensing*, vol. 8, no. 4, p. 354, 2016.
- [25] H. Gao, N. Zhang, and X. He, "A new integrated approach for water body extraction from high-resolution remote sensing imagery," *Remote Sensing Letters*, vol. 7, no. 8, pp. 745-754, 2016.
- [26] X. He, H. Weng, and Q. Li, "An automatic method for urban built-up area extraction using Landsat 8 OLI imagery," *Remote Sensing*, vol. 9, no. 10, p. 1000, 2017.
- [27] Y. Zhang, J. Zhang, and K. Zhang, "Monitoring vegetation dynamics by coupling the enhanced vegetation index and land surface temperature in karst areas of China," *Ecological Indicators*, vol. 72, pp. 128-138, 2017.
- [28] L. Jiang, J. Jiapaer, A. Bao, Y. Guo, and P. Ndayisaba, "Vegetation dynamics and responses to climate change and human activities in Central Asia," *Science of the Total Environment*, vol. 599-600, pp. 967-980, 2017.
- [29] A. P. Van Deventer, A. D. Ward, P. H. Gowda, and J. G. Lyon, "Using Thematic Mapper data to identify contrasting soil plains and tillage practices," *Photogrammetric Engineering and Remote Sensing*, vol. 63, no. 1, pp. 87-93, 1997.
- [30] Y. Chen, Y. Rao, and G. Yang, "Mapping bare soil using Sentinel-2 images based on the bare soil index: A case study in the Weihe River Basin, China," *Remote Sensing*, vol. 13, no. 6, p. 1124, 2021.
- [31] A. P. Andani, B. P. Hadian, and R. M. D. Prawira, "Land Suitability Analysis for Paddy Field Development in West Bandung Regency (Analisis Kesesuaian Lahan untuk Pengembangan Sawah di Kabupaten Bandung Barat)," *TATALOKA*, vol. 19, no. 3, pp. 139-151, 2017.
- [32] A. Firdaus, R. D. Listyaningrum, and A. H. Pratomo, "Paddy Field Conversion in Purwakarta Regency and Its Impact on Rice Production (Konversi Lahan Sawah di Kabupaten Purwakarta dan Pengaruhnya terhadap Produksi Padi)," *Indonesian Journal of Applied Science and Technology (InJAST)*, vol. 3, no. 2, pp. 101-111, 2022.
- [33] Politeknik Statistika STIS. 2022. "Mapping of Classification and Conversion of Agricultural Land Using Satellite Imagery (Pemetaan Klasifikasi dan Alih Fungsi Lahan Pertanian dengan Citra Satelit)". Laporan Hasil PKL 2021/2022 Nomor Buku 02 Riset 2.
- [34] Y. C. Putra, A. W. Wijayanto, and G. A. Chulafak, "Oil palm trees detection and counting on Microsoft Bing Maps Very High Resolution (VHR) satellite imagery and Unmanned Aerial Vehicles (UAV) data using image processing thresholding approach," *Ecological Informatics*, vol. 72, 2022, Art. no. 101878.
- [35] D. W. Triscowati, B. Sartono, A. Kurnia, D. D. Domiri, and A. W. Wijayanto, "Multitemporal remote sensing data for classification of food crops plant phase using supervised random forest," in *Proceedings of SPIE - The International Society for Optical Engineering*, vol. 11311, 2019, Art. no. 1131102.
- [36] M. Kadarisman, A. W. Wijayanto, and A. D. Sakti, "Government Agencies' Readiness Evaluation towards Industry 4.0 and Society 5.0 in Indonesia," *Social Sciences*, vol. 11, no. 8, Art. no. 331, 2022.